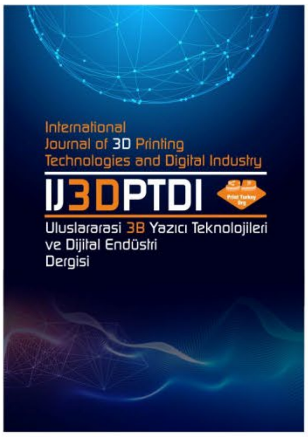

ULUSLARARASI 3B YAZICI TEKNOLOJİLERİ
VE DİJİTAL ENDÜSTRİ DERGİSİ

INTERNATIONAL JOURNAL OF 3D PRINTING
TECHNOLOGIES AND DIGITAL INDUSTRY

ISSN:2602-3350 (Online)
URL: https://dergipark.org.tr/ij3dptdi

OPTIMIZATION OF PROCESS PARAMETERS AND MECHANICAL PERFORMANCE OF GRAPHITE-REINFORCED PHOTOPOLYMER COMPOSITES FABRICATED VIA STEREOLITHOGRAPHY (SLA)

Yazarlar (Authors): Ali ÇAKAR*, Ömer SEÇGİN

Bu makaleye şu şekilde atıfta bulunabilirsiniz (To cite to this article): *Çakar A., Seçgin Ö., "Optimization of Process Parameters and Mechanical Performance of Graphite-Reinforced Photopolymer Composites Fabricated Via Stereolithography (SLA)" Int. J. of 3D Printing Tech. Dig. Ind., 10(1): 104-116, (2026).*

DOI: 10.46519/ij3dptdi.1837648

Araştırma Makale/ Research Article

Erişim Linki: (To link to this article): https://dergipark.org.tr/en/pub/ij3dptdi/archive

OPTIMIZATION OF PROCESS PARAMETERS AND MECHANICAL PERFORMANCE OF GRAPHITE-REINFORCED PHOTOPOLYMER COMPOSITES FABRICATED VIA STEREOLITHOGRAPHY (SLA)

Ali ÇAKAR[a,b] *, Ömer SEÇGİN[c]

[a] Sakarya University of Applied Sciences, Graduate Education Institute, TURKİYE
[b] FADA Engineering and Machinery Industry And Trade INC., TURKİYE
[c] Sakarya University of Applied Sciences, Technology Faculty, Mechanical Engineering Department, TURKİYE

* *Corresponding Author: 23500905001@subu.edu.tr*

(**Received:** 07.12.25; **Revised:** 21.01.26; **Accepted:** 06.03.26)

ABSTRACT

With the increasing demand for functional and high-performance materials in the manufacturing sector, improving the mechanical properties of polymer composites produced using Stereolithography (SLA) has gained importance. In this study, the mechanical performance of composite samples produced by adding graphite at different ratios (0.3%, 0.5%, and 0.7%) to photopolymer resin was experimentally investigated. The graphite addition ratio, layer thickness (0.05–0.1 mm), and light exposure time (4–6 s) were selected as variable parameters during the production process, and the experimental design was analyzed using Response Surface Methodology (RSM). The findings showed that production parameters have different effects on tensile and flexural strengths. Increasing the graphite content decreased tensile strength by causing discontinuities in the matrix structure, while increasing matrix stiffness improved flexural strength. Furthermore, reducing layer thickness and increasing curing time increased polymerization efficiency, which positively affected mechanical performance in both test groups. Optimization revealed that the ideal parameters for tensile strength were 0.3% graphite content, 0.05 mm layer thickness, and 6 s curing time, while a higher graphite content (0.7%) was found to be more effective for flexural strength. This study demonstrates the critical importance of parameter optimization based on the intended use (tensile or flexural priority) in SLA-based composite production.

Keywords: Stereolithography (SLA), Photopolymer Composite, Graphite, Additive Manufacturing

1. INTRODUCTION

Scientific and technological advances are leading to radical transformations in many sectors, particularly manufacturing, and are enabling the emergence of new production approaches. Within the context of Industry 4.0, technologies such as the internet of things, big data, cloud computing, cybersecurity, and autonomous robots have become fundamental components of modern production systems. Among these innovations, additive manufacturing is gaining increasing importance due to the design freedom, rapid production, and low-cost advantages it offers [1].

3D printing technologies are an innovative method that allows digitally created models to be transformed into physical objects through a layered structure [2]. Since the 1980s, additive manufacturing technologies have been used not only for prototyping but also for the manufacture of functional parts, offering significant advantages such as the ability to produce complex geometries without the need for molds, reducing material waste, and shortening production times [3–6]. Unlike traditional machining methods, additive manufacturing is based on the principle of adding material layer by layer only to the required areas. This simplifies the manufacturing process and significantly reduces design constraints. Methods such as SLA [7-8], FDM [9-10], SLS [11], and DLP [12] offer different performance characteristics depending on the material used and the final product requirements. The photopolymer-based SLA method, in particular, stands out for its high surface quality and precision [5,13].

VAT photopolymerization methods are based on the selective solidification of photosensitive liquid resins and are widely used in the production of high-resolution polymer parts. Among these technologies, stereolithography (SLA) stands out as one of the most advanced methods for producing superior accuracy, high surface quality, and complex geometries thanks to its layer-by-layer photopolymerization of resin using a scanning UV laser. These inherent advantages of SLA make the technology particularly desirable for applications requiring high precision, such as medical device manufacturing, automotive prototyping, and aerospace components [5,14].

Digital Light Processing (DLP) technology, which shares the same principle as SLA, uses a projector light source instead of a laser to cure the entire layer in one go, thus increasing production speed. However, due to projector-based imaging, it exhibits limited resolution compared to SLA. However, DLP offers an important alternative in time-critical applications thanks to its fast production advantage [5,15-16].

Continuous Liquid Interface Fabrication (CLIP), which aims to surpass the speed limits of layered photopolymerization, offers a layer-less production approach by continuously moving the resin pool downward. Production speeds approximately 100 times higher than traditional SLA/DLP processes can be achieved. This continuity in the process significantly increases production efficiency while maintaining high precision, creating the potential for industrial-scale use [5,17].

While the industrial use of additive manufacturing technologies is still limited, successful applications are seen in many sectors such as healthcare, aerospace, automotive, defense, mold making, and education. In Turkey, the widespread adoption of these technologies in industry is of strategic importance for the transition to high-technology production and the training of a qualified technical workforce [1].

In light of the articles examined, it is evident that studies on photopolymer composites exhibit significant differences in terms of the reinforcement material type (nano vs. micro/macro) and the targeted improvement mechanisms. The study by Shebeeb et al. focuses on the incorporation of carbon-based nanomaterials, such as graphene, into photopolymer matrices; they emphasize that while this approach results in superior mechanical and electrical properties, it creates serious challenges regarding curing depth due to graphene's UV light absorption (shielding effect) [18]. In contrast, the research by Trembecka-Wójciga and Ortyl concentrates on ceramic-filled photopolymers (ceramic slurries), noting that the primary challenge is managing resin viscosity under high solid loading rather than light absorption, and highlights the critical role of dispersants and surfactants as a solution [19]. Providing an application-oriented comparison, the study by Cafino et al [20]. reveals that photopolymer resins offer higher surface quality and detail precision in surgical modeling compared to thermoplastics like PETG (FDM), yet they may present disadvantages regarding cost and material brittleness. According to literature, while graphene-based composites aim to enhance the intrinsic functional properties (conductivity, strength) of the material, ceramic-filled systems utilize photopolymerization as a shaping tool for the production of final ceramic parts. Both methods require a greater degree of chemical compatibility (surface modification) and process optimization (curing time, viscosity control) compared to neat resins.

Research has shown that additive manufacturing technology offers an innovative solution to modern manufacturing processes thanks to its design flexibility, rapid production capacity, and sustainable approach. In the study discussed in this article, two different processes, the preparatory phase and the application phase, were considered as the effective factors. The aim of the study was to optimize the mechanical, electrical, and thermal properties of the samples against variable parameters by evaluating the produced sample samples and different test processes. In the first phase of the study, previous research in the literature was reviewed and it was determined that the amount of powdered graphite used in the graphite-added resin preparation processes was insufficient to create a homogeneous mixture, resulting in undesirable conditions such as agglomeration. Therefore, the amount of graphite used in the graphite-added resin preparation phase was reduced from 3% to 0.3%, thus ensuring homogeneity in the mixture. In SLA-type additive manufacturing applications using graphite-added resin in the application phase, key parameters affecting the mechanical properties of the samples were evaluated using not only the graphite additive ratio but also the light exposure time and layer thickness parameters. The findings indicate that, in addition to graphite addition, layer thickness and light exposure time are also decisive factors in determining the final properties of the material. This demonstrates the need for appropriate optimizations in production processes to achieve the desired properties.

2. MATERIALS AND METHODS

Test samples were produced by mixing the highly conductive oily graphite powder SC80/44 into the Anycubic Standard Resin (Clear) photopolymer resin. The samples were prepared according to ASTM D638 [21] Type I for tensile testing and ASTM D790 for flexural testing. The part production process was carried out using the Anycubic Photon Mono M5s Pro 3D printer. The mechanical properties of the produced samples were examined for tensile and flexural strength.

Anycubic Standard Resin (Clear), used in this study, is a photopolymer resin composed of acrylate-based oligomers and monomers that polymerizes under UV light using photoinitiators. Offering high surface quality and dimensional accuracy, this resin is a suitable material for detailed prototypes and engineering samples. Sample sets were produced within the scope of the experimental study by applying different exposure times, layer thicknesses, internal fill rates, and support structure types.

To determine mechanical performance, tensile and three-point bending tests were conducted using a 5-ton Shimadzu mechanical testing machine. This machine's high measurement precision, precise load-controlled testing capabilities, and data collection infrastructure in accordance with international standards enabled accurate determination of the mechanical properties of composite samples. The device's stable load application capability and precise elongation measurement systems in both tensile and bending tests allowed for a clear understanding of the effects of additive ratios and production parameters on material behavior.

The materials and test equipment used in the study were carefully selected to ensure the accuracy and reproducibility of the experimental process. The graphite additive used in composite production is commercial-grade SC80/44 graphite. This graphite has a carbon content of 80% and a size of 44 microns. It is classified as natural graphite. Its high purity, fine grain size, and homogeneous distribution ensure good dispersion within the photopolymer resin. These properties offer the potential to increase both mechanical strength and improve the thermal and electrical behavior of the polymer matrix within the composite structure. Standard Resin (Clear), a transparent photopolymer resin chosen as the matrix material, is known for its low viscosity suitable for the SLA process, its ability to produce high surface quality, and its rapid curing properties sensitive to UV light. This resin, when mixed with the additive, maintained its fluidity and curing stability, allowing for the stable operation of the production process.

An Anycubic Photon Mono M5s Pro SLA 3D printer was used to produce the samples. This device, thanks to its high-resolution 10.1-inch 14K monochrome display, can produce parts with high detail precision. It also ensures uniform curing between layers with its advanced light homogeneity technology [22]. Precise light control during the printing process facilitated stable solidification of the graphite-reinforced composite resin and allowed for reliable investigation of the effects of different layer thicknesses and light exposure times.

The methodology employed in this study was systematically planned to encompass all stages of the SLA-based composite sample fabrication process. In the first stage, the sample geometries to be used in mechanical testing were determined based on relevant standards and modeled in a CAD program. The digital designs were optimized for compatibility with the SLA fabrication process and converted to a suitable file format for transfer to the printer.

After the design phase, graphite-added composite resin mixtures were prepared. In this context, SC80/44 graphite powder was homogeneously mixed with the photopolymer Standard Resin (Clear) at predetermined ratios. A magnetic stirrer and controlled time methods were used to maintain the viscosity of the mixture suitable for SLA production. The mixing process was meticulously managed to prevent agglomeration or sedimentation within the resin due to the additive. Therefore, based on previous studies conducted with photopolymer-based resins [23-24], weight percentage (wt.%) ratios were used in the prepared resin mixtures to ensure homogeneity.

Printing parameters such as light exposure time, print layer thickness, and graphite ratio were selected from previous studies to determine the production process [18,25]. The experimental set was determined using the response surface method. In this analysis, the effect of a parameter or interaction on the response is evaluated according to the P (significance/probability) value. At a 95% confidence interval, i.e., when $P < 0.05$, the parameter is considered to have a significant effect on the response. However, the results show that no single parameter is a sole determinant. Instead, it appears that pairwise interactions between parameters have a stronger influence on the response. Parts were produced using the obtained experimental parameter combinations. Contour plots were drawn after the experiments to understand the effects of the parameters.

During the production phase, the prepared resin mixture was transferred to the Anycubic Photon Mono M5s Pro printer, and operating parameters were determined. Layer thickness and light exposure time were selected as variables due to the experimental design, and a total of 30 samples were produced to investigate the effects of these parameters. Samples were prepared in two sets of 15, as shown in Table 1. Each sample was prepared using the specified layer thicknesses and curing times ranging from 4 to 6 seconds, ensuring light homogeneity and printing stability throughout the production process [25-26].

Table 1. Experimental design matrix

Experiment No.	Mixing Ratio (%)	Layer Thickness (mm)	Light Exposure Time (sn)
1	0.5	0.1	6
2	0.5	0.1	4
3	0.5	0.075	5
4	0.3	0.05	5
5	0.3	0.075	4
6	0.5	0.075	5
7	0.7	0.075	4
8	0.5	0.05	6
9	0.7	0.075	6
10	0.7	0.05	5
11	0.5	0.05	4
12	0.3	0.075	6
13	0.5	0.075	5
14	0.7	0.1	5
15	0.3	0.1	5

After the samples were manufactured according to ASTM D638 [21], preparation for mechanical testing was carried out. The samples were first cleaned with isopropyl alcohol and then post-cured to stabilize their mechanical properties. During the testing phase, the fixtures and loading conditions required for the tensile and three-point bending tests were set on a Shimadzu 5-ton capacity mechanical testing machine, and each sample was tested with speed and load control parameters in accordance with the relevant standard. Using this systematic method, the effects of manufacturing parameters on mechanical performance were evaluated in a reliable and comparable manner. In the tensile test, the response of the samples to a force applied in the opposite direction at a tensile speed of 5 mm/s is measured using arms held at two points equidistant from the center of the sample. Tensile tests were conducted at room temperature. Images of the samples before and after the tensile test are shown in Figure 1.

Figure 1. Tensile test samples

Test specimens for the 3-point bending tests were manufactured in accordance with ASTM D790 [24] standards. The 3-point bending tests were conducted at room temperature and a speed of 5 mm/min. Bending tests were performed using a Shimadzu device capable of applying forces up to 5 tons.

In a three-point bending test, samples are supported by simple supports at two points, and a force is applied at the center of the sample from a third point. As the applied force increases, a deflection (D) occurs at the sample's midpoint. Meanwhile, bending stress occurs in the upper section of the cross-section, and tensile stress occurs in the lower section. The samples were placed in the testing machine with a support span of 60 mm. A vertical force was applied perpendicular to the center of the sample. Bending strength and bending modulus of elasticity were investigated in the three-point bending test. The bending modulus of elasticity indicates the flexibility of the material. If the material is flexible, the modulus of elasticity decreases. Figure 2 shows images from the beginning and during the experiment on the Shimadzu machine.

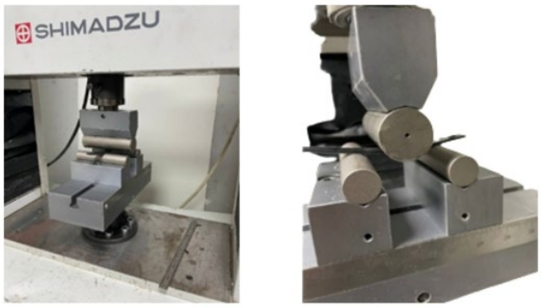

Figure 2. Bending test figures

In three-point bending tests, fracture occurs primarily in the lower fibers of the sample. This is primarily due to the fact that the tensile strength of materials is generally lower than their flexural strength. Under these loading conditions, the maximum bending stress occurs at the midpoint on the lower surface of the sample and is calculated using Equation 1.

$$\sigma = \frac{3PL}{2bd^2} \quad (1)$$

The quantities used in the equation are defined as follows: σ (sigma) represents the bending stress and its unit is N/mm². P is the force applied to the midpoint of the sample during the test and is expressed in Newtons (N). L indicates the distance between supports and represents the opening of the sample between two supports, in millimeters (mm). b represents the width of the bending test sample, and d represents the height of the sample section, both in millimeters (mm). These quantities are used to calculate the bending stress on the sample and the resulting deformation behavior.

The flexural strength at fracture is obtained by applying the maximum force borne by the sample to the equation. If the material does not fracture but undergoes plastic deformation, the flexural yield stress is calculated using the force P value corresponding to the yield zone.

The flexural strain occurring at the midpoint on the lower surface of the sample is calculated using Equation 2 using the maximum deflection value D. This expression represents the theoretical description of the strain distribution that occurs depending on the geometry and deflection behavior of the section under bending.

$$\varepsilon = \frac{6Dd}{L^2} \quad (2)$$

3. FINDINGS

In this study, two different mechanical test results were analyzed: a tensile test and a 3-point bending test. These analyses were performed using Minitab software and presented comparatively in contour plots.

3.1. Tensile Test Results

Tensile tests performed on graphite-added samples using the SLA method revealed a comprehensive evaluation of the effects of production parameters (mixture ratio, layer thickness, and light exposure time) on tensile strength using both tables and contour plots. Table 2 below presents the tensile strength test results for samples produced using the SLA method, along with the combinations of graphite addition ratio, layer thickness, and light exposure time.

Table 2. Experimental results

Exp. No.	Mix. Ratio (%)	Layer Thick. (mm)	Light Exp. Time (sn)	Tensile Strength (N/mm^2)	Bending Strength (N/mm^2)
1	0.5	0.1	6	23.6	18.45
2	0.5	0.1	4	23.29	21.1
3	0.5	0.075	5	18.54	19.38
4	0.3	0.05	5	33.42	39.7
5	0.3	0.075	4	15.52	15.68
6	0.5	0.075	5	13.37	24.9
7	0.7	0.075	4	19.08	19.38
8	0.5	0.05	6	26.95	21.22
9	0.7	0.075	6	19.3	19.38
10	0.7	0.05	5	18.11	30.45
11	0.5	0.05	4	18.43	32.29
12	0.3	0.075	6	18.87	25.84
13	0.5	0.075	5	25.12	27.68
14	0.7	0.1	5	21.78	23.07
15	0.3	0.1	5	19.51	22.14

When the experimental results presented in Table 2 are examined, it is clearly seen that increasing the graphite content causes a general decrease in tensile strength. This is also strongly confirmed in the contour plots. Graphene agglomerations formed during part production accelerate fracture by creating weak areas, while graphene-polymer interactions reduce the flexibility of the material by restricting the movement of the polymer chains. Examining the contour plot in Figure 3, the significant decrease in strength as the graphite content increases indicates that graphite weakens the load transfer mechanism within the resin matrix and creates discontinuities between the polymer chains [24,27-28]. Based on samples 4 and 15 in Table 2, it is observed that increasing layer thickness, like increasing graphite content, adversely affects tensile strength and reduces it. Figure 3's contour plot illustrates the inverse relationship between layer thickness and mixing ratio and tensile strength.

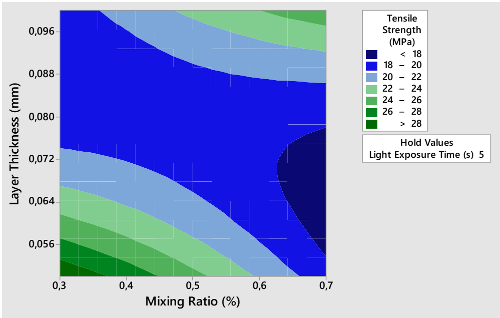

Figure 3. Tensile strength test: contour plot of layer thickness and mixing ratio

Literature indicates that increasing the curing time in SLA-based additive manufacturing processes results in more homogeneous microstructures and reduces cracking [29]. Studies on photopolymer-based resins containing graphite support the idea that these materials, which can significantly absorb UV light, can significantly affect the effect of light exposure time on mechanical properties [18,23]. However, as can be seen in Table 2, when comparing samples 1 and 2, as well as samples 5 and 12, increasing the light exposure time significantly increased the tensile strength at low graphite content. In other words, it was observed that longer curing times completed the polymerization and improved mechanical performance. However, the same effect was limited at higher content, i.e., samples 1 and 2. This can be explained by the difficulty in light penetration with increasing graphite density and the weakening of homogeneous bonding in the matrix. As can be seen in the contour plot of mixing ratio versus light exposure time given in Figure 4, higher tensile strengths can be obtained by increasing the light exposure time at low mixing ratios.

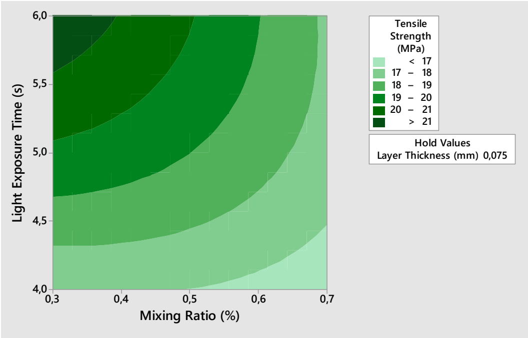

Figure 4. Tensile strength: light exposure time and mixing ratio contour plot

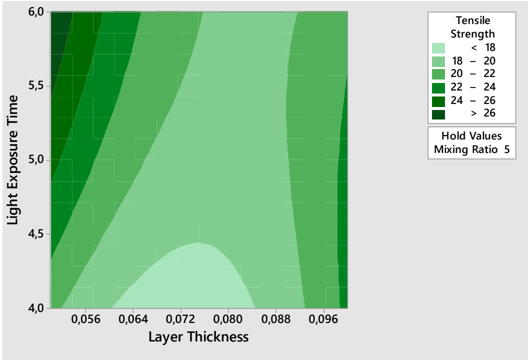

Figure 5. Tensile strength: contour plot of light exposure time and layer thickness

In the contour graph shown in Figure 5, layer thickness and light exposure time can be evaluated together. It can be seen from this graph that polymerization depth and interlayer bonding quality, which are critical in SLA production processes, are the primary factors determining tensile strength. With short light exposure times, resins fail to fully cure and their effects on mechanical strength are reduced, while high light exposures do not produce any significant change [23,24]. However, considering the changes in layer thickness and light transmittance, it is clear that these two parameters need to be optimized relative to each other. Because light can spread more effectively and homogeneously in thin layers, it has been observed that strength increases with longer light exposure times. Conversely, as layer thickness increases, the effectiveness of light reaching the lower layers decreases. This leads to both curing instability and a decrease in interlayer bonding quality, reducing tensile strength. This situation is more evident in Figure 5. Tensile strength decreases to its lowest levels in regions where high graphite content meets high layer thickness. This dual effect can be explained by the overlapping effects of both insufficient polymerization due to layer thickness and the negative impact of graphite additives on structural integrity. Another point to note is that, when increasing layer thickness, tensile strength, which is expected to decrease after a certain thickness, increases. However, it was observed that the highest tensile strength values were achieved at low layer thicknesses and high light exposure times. Considering these data, optimization studies were conducted for three variables.

Upon examining the contour plot presented in Figure 5, it is evident that mechanical strength is strongly dependent on the interaction between layer thickness and light exposure time. The highest strength values (indicated by darker regions) were achieved at the combination of minimum layer thickness (0.05 mm) and maximum light exposure time (6 s).

This behavior can be rationalized by photopolymerization kinetics and the Beer-Lambert law. As the layer thickness increases, the penetration depth of UV light diminishes due to the 'shielding effect' of the graphite particles within the resin, leading to insufficient polymerization at the bottom surfaces of the layers. At low layer thicknesses (0.05 mm), light energy is distributed more homogeneously throughout the layer, ensuring full conversion and enhancing interlayer bonding. Conversely, at greater layer thicknesses (0.1 mm) combined with low exposure times (4 s), the inability of the resin to fully cure results in the formation of 'undercured regions,' which introduce structural weaknesses and significantly reduce mechanical strength.

In this study, optimal parameter levels were determined by performing response surface optimization. This optimization result is fully consistent with the trends observed in the contour plots. The combination of a low graphite content of 0.3%, a low layer thickness of 0.05 mm, and a medium-high light exposure time of 6 seconds were found to be the production conditions that maximized tensile strength. This is consistent with both chemical factors arising from the material-graphite resin interaction and characteristic effects such as layer polymerization behavior during the production process.

When all data obtained from the contour plots, optimization analysis, and test table are evaluated together, it is seen that the effects of production parameters on tensile strength hierarchically reinforce each other. The parameter that most significantly affects tensile strength is the graphite mixture ratio, followed by layer thickness and light exposure time. These findings demonstrate that production parameters must be meticulously controlled to optimize the processability and mechanical performance of graphite-added polymer composites in the SLA method. Considering the interactions between the parameters, it is clearly demonstrated that a low graphite ratio and thin-layer production strategy, when supported by sufficient light exposure time, yield the most effective results in terms of tensile strength.

3.2. Bending Test Results

The results of the three-point bending tests are presented in Table 2. An examination of the table reveals that changes in the parameters have a significant impact on flexural strength. In particular, decreasing layer thickness and increasing light exposure time significantly increased flexural strength, allowing the polymer to cure more homogeneously within the matrix. However, at higher mixing ratios, the graphite addition was observed to support the bond strength between polymer chains and increase strength.

The contour plot in Figure 6 shows the change in flexural strength depending on the mix ratio and light exposure time. An examination of the plot reveals a significant improvement in flexural strength with increasing light exposure time, but this effect varies depending on the mix ratio. While strength increases more limitedly at lower mix ratios, strength reaches much higher values as the mix ratio increases to 0.7%. This demonstrates that the graphite additive has a supportive effect on light-curing efficiency. The dark green areas concentrated on the plot indicate the optimum parameter range.

Figure 7 shows the change in flexural strength with layer thickness and light exposure time in the contour plot. The graph shows that decreasing the layer thickness (0.05 mm and below) significantly increases the flexural strength. This is mainly because in thinner layers, the bonding between successive layers is more homogeneous and the curing reaction is more efficient. Furthermore, it is observed that the strength reaches the highest levels when the light exposure time approaches 6 seconds. However, as the thickness approaches 0.1 mm, the strength decreases rapidly. This effect is clearly seen in the regions where blue tones dominate the contour map. In regions where the layer thickness approaches 0.1 mm (Figure 7, upper right corner), the flexural strength decreases to the level of 40 MPa. These results support the idea that increasing the light exposure time increases the strength by curing the composite better, making it brittle. However, in thicker layers, it reduces both strength and flexibility due to the formation of voids during printing [24,30–32].

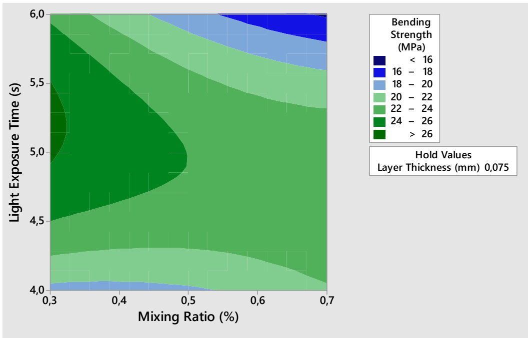

Figure 6. Flexural strength: light exposure time and mixing ratio contour plot

The decisive impact of light exposure time on mechanical performance is intrinsically linked to the degree of conversion and cross-linking density within the composite structure. While UV irradiation can penetrate unobstructed to a specific depth (penetration depth) in neat photopolymer resins, the incorporation of graphite particles into the matrix drastically alters optical transmittance. Due to their opaque nature and large surface areas, carbon-based fillers exhibit a strong tendency to absorb and scatter UV radiation, a phenomenon described in the literature as the "shielding effect" [23-24]. Graphite particles intercept photons required for the activation of photoinitiators, thereby hindering light penetration into deeper resin layers and limiting the cure depth in accordance with the Beer-Lambert law. Consequently, under insufficient light exposure, unpolymerized or partially cured monomer regions remain surrounding the graphite particles, which compromises the structural integrity of the matrix and degrades mechanical strength [23]. In this study, the improvement observed in mechanical properties with the increase in exposure time (from 4 to 6 s) can be attributed to compensating for this optical shielding induced by graphite and achieving a higher polymerization conversion rate. Prolonged exposure times ensured that sufficient energy reached the lower layers despite the masking effect, thereby enhancing interlayer covalent bonding.

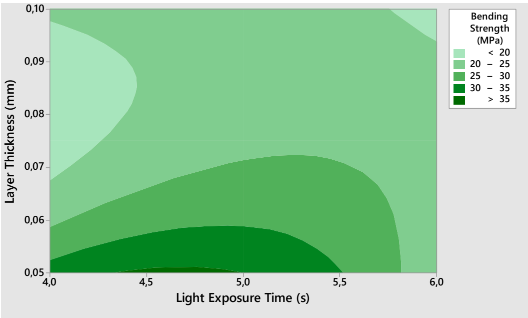

Figure 7. Flexural strength: light exposure time and layer thickness contour plot

Upon examining the contour plot illustrating the variation of flexural strength with layer thickness and light exposure time (Figure 7), it is evident that these two parameters have a significant interaction effect on mechanical performance. The highest strength values in the plot are concentrated in the region where layer thickness is reduced to the 0.05 mm level and light exposure time approaches 6 seconds.
This phenomenon can be explained by the critical balance between cure depth and layer thickness during the photopolymerization process. Increasing the layer thickness (to 0.1 mm) hinders the penetration of UV light within the resin, and when combined with the light-absorbing effect of graphite particles, leads to the formation of undercured regions between layers. Insufficient curing weakens interlayer bonding, increasing the risk of delamination under flexural loads and reducing strength. Conversely, the combination of low layer thickness and high exposure time enhances the degree of conversion, promoting the formation of a more homogeneous and rigid cross-linked structure, thereby maximizing flexural strength.

The contour plot in Figure 8 illustrates the effects of layer thickness and mix ratio on flexural strength. This plot demonstrates that the combination of low layer thickness and high mix ratio provides the most advantageous strength. As the mix ratio increases, the graphite particles contribute to the load-carrying capacity and increase the rigidity of the matrix structure. However, as layer thickness increases to 0.075 mm or more, the effectiveness of this contribution decreases. Therefore, it appears that low layer thickness and high mix ratio should be applied simultaneously for optimum flexural strength.

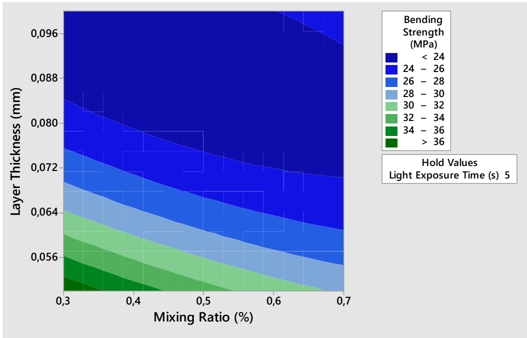

Figure 8. Flexural strength: test layer thickness and mixing ratio contour graph

Optimum parameter levels (maximizing flexural strength) were determined by optimization using the response surface method. Based on the optimization results, the optimum values were determined as follows: a mixing ratio of 0.07%, a layer thickness of 0.05 mm, and a light exposure time of 5 s.

With this parameter set, the flexural strength reaches approximately 71.55 MPa, representing the highest level of experimental results. An examination of the factors reveals that the contribution of each parameter to flexural strength exhibits a non-linear trend. In particular, even small changes in layer thickness have significant effects on strength.

The most prominent finding of this study is the dual effect of graphite addition on the mechanical behavior of the composite structure, where it significantly improves flexural strength while weakening tensile strength. The reduction in tensile strength is primarily attributed to structural discontinuities within the polymer matrix and weak interfacial interaction between the graphite particles and the matrix; these regions act as stress concentration points under tensile loading, facilitating crack propagation [28]. Conversely, the increase observed in flexural tests is associated with the high elastic modulus and stiffness of graphite. Under the compressive stresses generated on the upper cross-section of the specimen during bending, the graphite fillers function as a stiffening phase, restricting plastic deformation and enhancing the load-bearing capacity of the matrix [27,31]. This result aligns with recent studies reporting that carbon-based fillers can enhance compressive and flexural moduli while limiting tensile strength due to interfacial challenges [24].

Following the tensile test, SEM images of sample 10 are given in Figure 9. This sample was produced with a mixing ratio of 0.7, a layer thickness of 0.05, and a light exposure time of 5 seconds. The tensile strength of this sample was found to be 18.11 MPa, and its flexural strength was 71.55 MPa.

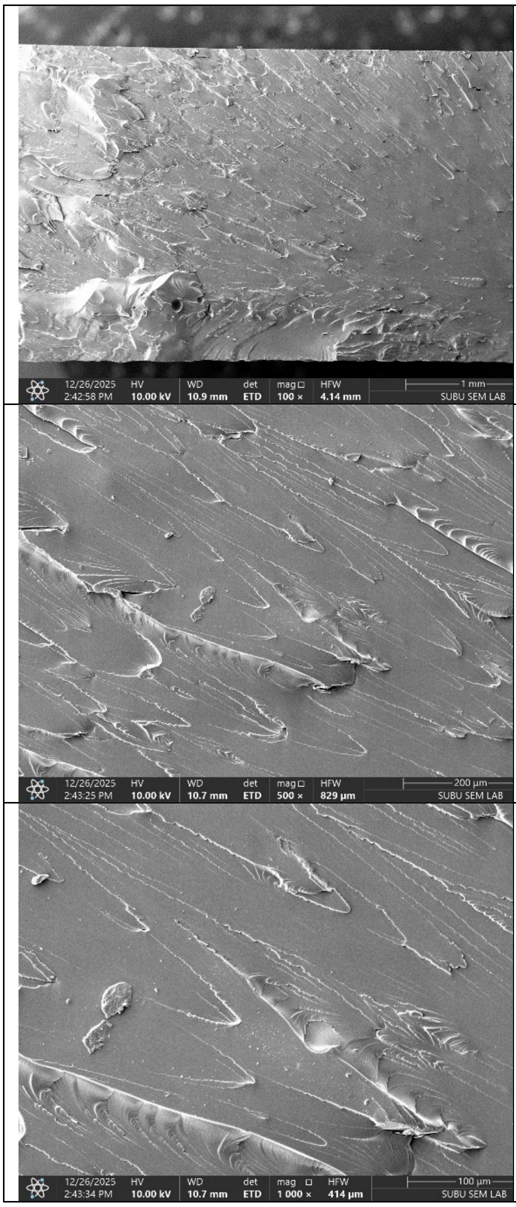

A

B

C

Figure 9. SEM images of sample number 10. A) 100x, B) 500x, C) 1000X

Figure 9.A shows the image obtained at 100x magnification, Figure 9.B at 500x magnification, and Figure 9.C at 1000x magnification. A stable distribution was observed on the surface in the SEM images. A distinct and layered peeling was observed in the direction of flow, along the direction of the tensile test. The effects of the deformation were visualized as interlayer separation. No agglomeration or other graphite accumulation was observed on the part surface.

4. RESULTS

In this study, the effects of graphite addition ratio (0.3% - 0.7%), layer thickness (0.05 - 0.1 mm), and light exposure time (4 - 6 s) on the mechanical performance of photopolymer composites produced by SLA-based additive manufacturing method were investigated experimentally and optimized using response surface methodology (RSM). In the light of the findings, the following basic conclusions were reached:

- Due to the discontinuity and weak interfacial bonding created by graphite particles within the matrix, a decrease in tensile strength was observed as the additive content increased. However, this decrease could be limited by optimizing the production parameters. Optimum conditions were determined to be 0.3% graphite content, 0.05 mm layer thickness, and 6 s curing time; a maximum tensile strength of 33.42 MPa was achieved with this parameter set. This value represents an approximately 150% performance increase compared to the sample with the lowest strength (13.37 MPa).

- Unlike the tensile test, graphite addition positively affected flexural strength. Thanks to the graphite particles' ability to support matrix stiffness under load, superior mechanical properties were achieved at higher addition rates. Optimization yielded a maximum flexural strength of 71.55 MPa with a 0.7% graphite content, 0.05 mm layer thickness, and a 5-sec curing time. This result represents a 94% improvement over the lowest flexural strength combination (36.86 MPa).

- For both test groups, reducing the layer thickness (0.05 mm) and increasing the curing time were the most critical factors to improve the mechanical performance by increasing the degree of polymerization and the quality of interlayer bonding.

- The study results highlight the need for customized production strategies tailored to the application area. A low graphite content (0.3%) should be preferred for parts requiring high flexibility and tensile strength, while a high graphite content (0.7%) yields more effective results for body parts where rigidity and bending resistance are critical.

The study determined that the mechanical performance of graphite-added photopolymer composites is highly sensitive to production parameters. The effect of graphite additive varies depending on the loading type, with lower additive concentrations being more advantageous for tensile strength, while higher additive concentrations yielded more favorable results for flexural strength. Reducing layer thickness and increasing light exposure time were identified as common parameters that improved mechanical performance in both tensile and flexural tests. In conclusion, optimal mechanical performance in the production of graphite-added composite materials using the SLA method is achieved by correctly selecting the production parameters. The best results obtained in the study demonstrate that different strategies can be preferred depending on the intended use of the material. To address the matrix-reinforcement incompatibility, which is the primary cause of the decrease in tensile strength caused by graphite additive, future studies are recommended to apply surface modification to graphite particles using silanization or similar methods and to conduct research on increasing interfacial bond strength.

The obtained experimental data reveal that graphite-reinforced SLA composites offer 'tunable' mechanical performance for industrial applications. In particular, the high flexural strength and increased matrix rigidity achieved with 0.7% graphite addition enhance the potential of these composites for manufacturing structural components exposed to bending and compressive loads, such as brackets, electronic circuit housings, or unmanned aerial vehicle (UAV) fuselage parts. Conversely, processes optimized with low additive ratios (0.3%) present a more suitable solution for snap-fits and precise functional prototypes where material continuity and tensile strength are critical. In this context, the study demonstrates that by optimizing production parameters according to the intended end-use, SLA technology can evolve beyond being merely a visual modeling tool to play an active role in the manufacturing of load-bearing end-use products.

ACKNOWLEDGMENTS

We extend our gratitude to the Scientific Research Projects Coordination Unit (BAPK) of Sakarya University of Applied Sciences for providing support to project number 313-2025 in the execution of this study.

REFERENCES

1. Özsoy, K., Duman, B., "Usability Of Additive Manufacturing (Three Dimensional Printing) Technologies In Education", International Journal Of 3d Printing Technologies And Digital Industry, Vol 1. , Pages 36–48, 2017.

2. Seçgin, Ö., Arda, E., Ata, E., Çelik, H.A., "Dimensional Optimization of Additive Manufacturing Process", Journal of the Chinese Society of Mechanical Engineers, Transactions of the Chinese Institute of Engineers, Series C/Chung-Kuo Chi Hsueh Kung Ch'eng Hsuebo Pao, Vol. 43, Issue 1, Pages 75–8, 2022.

3. Ryan, K.R., Down, M.P., Hurst, N.J., Keefe, E.M., Banks, C.E., "Additive manufacturing (3D printing) of electrically conductive polymers and polymer nanocomposites and their applications", eScience, Vol. 2, Issue 4, Pages 365–81, 2022.

4. Delgado Camacho, D., Clayton, P., O'Brien, W.J., Seepersad, C., Juenger, M., Ferron, R., et al., "Applications of additive manufacturing in the construction industry – A forward-looking review", Automation in Construction, Vol. 89 (August 2017), Pages 110–9, 2018.

5. Kim, H., Kim, K.H., Jeong, J., Lee, Y., Jung, I.D., "Recent progress on materials for functional additive manufacturing", Materials Science in Additive Manufacturing, Vol. 3, Issue 2, Pages 3323–49, 2024.

6. Groover, M.P., "Automation, Production Systems, and Computer-Integrated Manufacturing", 2000.

7. Schmidleithner, C., Kalaskar, D.M., "Stereolithography", InTech; 2018.

8. Han, K., Aktaş, N.F., "Properties and Applications of Resin Types Used in Sla 3D Printers", In: Pioneer And Innovative Studies In Engineering All Sciences Academy; 2024.

9. Melnikova, R., Ehrmann, A., Finsterbusch, K., "3D printing of textile-based structures by Fused Deposition Modelling (FDM) with different polymer materials", IOP Conference Series: Materials Science and Engineering, Vol. 62, Issue 1, Pages 12018–25, 2014.

10. Taşdemir, V., "Investigation of the Effects of the Number of Shells, Raster Angle, Extrusion Ratio, and Path Width on Printed Polylactic Acid Parts with Fused Deposition Modeling 3D Printer", Journal of Materials Engineering and Performance, Vol. 33 , Pages 11888–11898, 2024.

11. Fina, F., Goyanes, A., Gaisford, S., Basit, A.W., "Selective laser sintering (SLS) 3D printing of medicines", International Journal of Pharmaceutics, Vol. 529, Issue 1–2, Pages 285–93, 2017.

12. Valentinčič, J., Peroša, M., Jerman, M., Sabotin, I., Lebar, A., "Low cost printer for DLP stereolithography", Strojniski Vestnik/Journal of Mechanical Engineering, Vol. 63, Issue 10, Pages 559–66, 2017.

13. Frazier, W.E., "Metal additive manufacturing: A review", Journal of Materials Engineering and Performance, Vol. 23, Issue 6, Pages 1917–28, 2014.

14. Akın, Y., Han, K., Tüylü, A., Aktaş, N.F., Çobaner, S., Çerlek, Ö., et al., "Compressive strength and performance of horizontally and vertically oriented hybrid lattice structures manufactured by stereolithography", Proceedings of the Institution of Mechanical Engineers, Part E: Journal of Process Mechanical Engineering, 2025.

15. Chiappone, A., Fantino, E., Roppolo, I., Lorusso, M., Manfredi, D., Fino, P., et al., "3D Printed PEG-Based Hybrid Nanocomposites Obtained by Sol-Gel Technique", ACS Applied Materials and Interfaces, Vol. 8, Issue 8, Pages 5627–33, 2016.

16. Sürmen, H.K., "Additive Manufacturing (3D Printing): Technologies and Applications", Uludağ University Journal of The Faculty of Engineering, Vol. 24, Issue 2, Pages 373–92, 2019.

17. Wang, W., Liu, S., Liu, L., Alfarhan, S., Jin, K., Chen, X., "High-Speed and High-Resolution 3D Printing of Self-Healing and Ion-Conductive Hydrogels via μCLIP", ACS Materials Letters, Vol. 5, Issue 6, Pages 1727–37, 2023.

18. Shebeeb, C.M., Afif, M. Bin, Jacob, L., Choi, D., Butt, H., "Vat photopolymerisation 3D printing of graphene-based materials", Virtual and Physical Prototyping, Vol. 18, Issue 1, Pages 1745–67, 2023.

19. Trembecka-Wójciga, K., Ortyl, J., "Enhancing 3D printed ceramic components: The function of dispersants, adhesion promoters, and surface-active agents in Photopolymerization-based additive manufacturing", Advances in Colloid and Interface Science, Vol. 332 (June)2024.

20. Cafino, R., Soliven, M.M.T., Velasco, L.C., Lopez, K.H., "Evaluation of polyethylene terephthalate glycol (PETG), SimuboneTM, and photopolymer resin as 3D printed temporal bone models for surgical simulation", Asian Journal of Surgery, Vol. 47, Issue 1, Pages 237–44, 2024.

21. ASTM., "Test Method for Tensile Properties of Plastics", Vol. D638 − 14, ASTM International. 2014.

22. Çerlek, Ö., Kesercioğlu, M.A., Han, K., "Stereolithography (SLA): An Innovative Additive Manufacturing Process", In: New Trends and Frontiers in Engineering All Sciences Academy; 2024.

23. de Armentia, S.L., Fernández-Villamarín, S., Ballesteros, Y., Real, J.C. de., Dunne, N., Paz, E., "3D Printing of a Graphene-Modified Photopolymer Using Stereolithography for Biomedical Applications: A Study of the Polymerization Reaction", International Journal of Bioprinting, Vol. 8, Issue 1, Pages 182–97, 2022.

24. Aldhanhani, S., Ali, M., Elkaffas, R.A., Butt, H., Samad, Y.A., "Advancing Structural Integrity: Graphene Nanocomposites via Vat Photopolymerization 3D Printing", ES Materials and Manufacturing, Vol. 26 , Pages 1–14, 2024.

25. Farkas, A.Z., Galatanu, S.V., Nagib, R., "The Influence of Printing Layer Thickness and Orientation on the Mechanical Properties of DLP 3D-Printed Dental Resin", Polymers, Vol. 15, Issue 5, Pages 1113–27, 2023.

26. Taranath, T.P., Varun, K.S., Thimmegowda, M.B., "Effect of Layer Thickness on the Tensile and Impact Behaviour of SLA-Printed Parts", International Journal for Research in Applied Science and Engineering Technology, Vol. 12, Issue 11, Pages 1848–52, 2024.

27. Li, Y., Wang, S., Wang, Q., "Enhancement of tribological properties of polymer composites reinforced by functionalized graphene", Composites Part B: Engineering, Vol. 120 , Pages 83–91, 2017.

28. Papageorgiou, D.G., Li, Z., Liu, M., Kinloch, I.A., Young, R.J., "Mechanisms of mechanical reinforcement by graphene and carbon nanotubes in polymer nanocomposites", Nanoscale, Vol. 12, Issue 4, Pages 2228–67, 2020.

29. Alshamrani, A.A., Raju, R., Ellakwa, A., "Effect of Printing Layer Thickness and Postprinting Conditions on the Flexural Strength and Hardness of a 3D-Printed Resin", BioMed Research International, Pages 1–9, 2022.

30. Rankouhi, B., Javadpour, S., Delfanian, F., Letcher, T., "Failure Analysis and Mechanical Characterization of 3D Printed ABS With Respect to Layer Thickness and Orientation", Journal of Failure Analysis and Prevention, Vol. 16, Issue 3, Pages 467–81, 2016.

31. Feng, Z., Li, Y., Hao, L., Yang, Y., Tang, T., Tang, D., et al., "Graphene-reinforced biodegradable resin composites for stereolithographic 3D printing of bone structure scaffolds", Journal of Nanomaterials, 2019 , Pages 1–13, 2019.

32. Ayrilmis, N., Kariz, M., Kwon, J.H., Kitek Kuzman, M., "Effect of printing layer thickness on water absorption and mechanical properties of 3D-printed wood/PLA composite materials", International Journal of Advanced Manufacturing Technology, Vol. 102, Issue 5–8, Pages 2195–200, 2019.